Research Paper
Computational Methods for Differential Equations
http://cmde.tabrizu.ac.ir
Vol. *, No. *, *, pp. 1-15
DOI:10.22034/cmde.2026.68757.3353

Effective control of quarantine of infected individuals in reducing the spread of contagious diseases

Raziyeh Choobineh, Haji Mohammad Mohammadi Nejad*, and Omid Rabiei Motlagh

Department of Mathematics, Faculty of Mathematical Sciences and Statistics, University of Birjand, Birjand, Iran.

Abstract

Our primary objective is to develop a regulated mathematical model for studying the dynamics of communicable disease transmission. By implementing a control that minimizes a cost function, considering the impacts of the illness as well as the costs associated with control, health, and quarantine measures, we aim to reduce the number of infections. To evaluate the effectiveness of the control, we will compare the outcomes of both uncontrolled and controlled scenarios. We will also analyze key characteristics of the model concerning threshold values, investigating aspects such as the boundaries and positivity of the solutions within a biological context. Additionally, we will assess the local and global behavior of the system about its equilibrium points.

Keywords. Contagious Diseases, Pontryagin's Maximization Principle, COVID-19.
2010 Mathematics Subject Classification. 92B10, 49J15.

1. Introduction

Infectious diseases have significantly impacted human history. In 2019, the first cases of COVID-19 were reported in Wuhan, China. The disease began to spread globally in March 2020, prompting the World Health Organization (WHO) to declare it a global pandemic [12]. Some researchers suggest that bats may carry the coronavirus, which could have been transmitted to humans. The initial patients were all linked to wet markets in Wuhan, but the infection quickly spread worldwide within a few months. Today, society continues to face challenges due to the pandemic [3]. Since then, extensive efforts have been made to understand the dynamics of the pandemic and to develop effective control strategies.

Mathematical modeling serves as a powerful tool to simulate and analyze the impacts of various interventions [5]. It enables policymakers to make informed decisions regarding resource allocation and the timing of control measures. This includes evaluating different vaccination strategies, such as targeted versus mass vaccination, determining appropriate quarantine durations, and assessing the effectiveness of public health measures like mask-wearing and social distancing in the absence of pharmaceutical treatments. Furthermore, these models can be used to forecast the likelihood of future outbreaks and identify vulnerable populations that require prioritized attention. By integrating epidemiological data, economic considerations, and behavioral insights, mathematical models can significantly contribute to the development of robust and cost-effective disease control strategies. Ultimately, this contributes to improved public health outcomes and fosters a more resilient society in the face of future pandemics.

The first mathematical model of an infectious disease was proposed by Daniel Bernoulli in 1760. Since then, numerous researchers have made significant contributions to this field. These evolving models help clarify the mechanisms of disease transmission and the effectiveness of various control strategies. In 2020, Eikenberry and colleagues investigated the impact of using face masks to prevent the spread of the COVID-19 pandemic, highlighting their crucial role in reducing transmission [4]. Additionally, Anwar Zeb and his team presented a SIR epidemic model that illustrates how

Received: 21 August 2025; Accepted: 25 May 2026.
∗ Corresponding author. Email: hmohammadin@birjand.ac.ir.

the spread of the disease is influenced by the number of infected individuals relative to the susceptible population and how it is transmitted through contact.

Isa Abdullahi Baba et al. (2021) introduced a SIR epidemic model in Nigeria to examine the rates of increase and decrease of a disease among different states of infected and susceptible individuals, both in quarantine and non-quarantine scenarios. Their findings indicated that implementing quarantine measures and restrictions for both susceptible and infected groups effectively reduced the incidence of the disease [7].

Abdullahi Saeed Ahmed et al. (2020) examined the SHIQ epidemic model across various states, including the disease-free equilibrium (DFE) and endemic states [1]. In addition, Musa et al. (2021) explored a mathematical model that incorporated awareness programs and different hospitalization strategies for both mild and severe cases, assessing the impact of these initiatives [9].

One of the main concerns regarding any infectious disease is how it spreads and how common it becomes in the community. A key measure in epidemiology is the basic reproduction number, denoted as R_0. This value indicates the average number of new cases caused by an infected person in a fully susceptible population. Therefore, implementing effective control strategies is crucial to lowering R_0 and managing outbreaks successfully.

This paper explores the dynamics of COVID-19 spread, focusing on transmission methods and the crucial role of quarantine strategies in mitigating it. Our primary objective is to develop optimal control strategies that minimize both the spread of infections and the costs associated with healthcare interventions. The main model presented in this paper is based on a recent study by Abdullah et al. [1], which, for the first time, claims to examine the interactions among four population groups: the susceptible population (S), the healthy population (H), the infected population (I), and the quarantined population (Q).

$$\begin{cases} \dfrac{dS(t)}{dt} = \Lambda - aS(t)I(t) - A_1S(t), \\ \dfrac{dH(t)}{dt} = b - cH(t)I(t) + \beta I(t) - A_1H(t), \\ \dfrac{dI(t)}{dt} = aS(t)I(t) + cH(t)I(t) + \alpha Q(t) - (A_1 + \gamma + \beta)I(t), \\ \dfrac{dQ(t)}{dt} = \gamma I(t) - (A_1 + \alpha)Q(t). \end{cases} \tag{1.1}$$

The $SHIQ$ model [1] was employed to analyze epidemic dynamics. The authors calculated the basic reproduction number and established sufficient conditions for the stability of the infection-free subsystem. The SHIQ epidemic model [1] serves as a framework for examining the dynamics of COVID-19, including situations where the system is subjected to control measures. In this study, we apply optimal control to the system described in Equation (1.1) and consider the following:

$$\begin{cases} \dfrac{dS(t)}{dt} = \Lambda - a(1-u(t))S(t)I(t) - A_1S(t), \\ \dfrac{dH(t)}{dt} = b - c(1-v(t))H(t)I(t) + \beta I(t) - A_1H(t), \\ \dfrac{dI(t)}{dt} = a(1-u(t))S(t)I(t) + c(1-v(t))H(t)I(t) + \alpha Q(t) - (A_1 + \gamma + \beta)I(t), \\ \dfrac{dQ(t)}{dt} = \gamma(1+w(t))I(t) - (A_1 + \alpha)Q(t). \end{cases}$$

Figure 1 shows the block diagram of the controlled model. These controls, illustrated in the model's structure Figure 1, aim to reduce disease spread and mortality, as well as increase the effectiveness of quarantine programs. As we will see, their efficacy must be optimized by minimizing a cost function that monitors the program's total cost. We are also interested in their influence on the basic reproduction number R_{0c} due to its theoretical importance. The COVID-19 pandemic highlighted the need for such well-defined, cost-effective disease control strategies to improve program effectiveness, given the costly quarantine and mass vaccination measures implemented.

The paper is organized as follows: First, the next section provides a summary and corrects minor miscalculations found in the results of [1]. This correction is crucial because the control strategy presented in this paper is applied

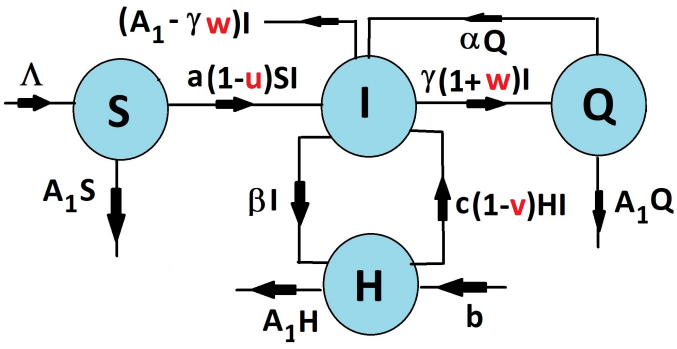

FIGURE 1. Block diagram for the control model. The jets marked on the paths indicate the direction of movement of people in the model compartments. As can be seen, the controls implemented will reduce the infection rate of individuals, along with the death rates of sick people, and improve quarantine policies.

to Equation (1.1), and any inaccuracies in [1] could jeopardize the comparison between the device's controlled performance and the uncontrolled experimental results. In section 3, we will utilize Pontryagin's maximization principle to derive a precise optimal control strategy that includes measures such as quarantine, vaccination, and health awareness campaigns aimed at significantly reducing infection rates. Additionally, we will implement targeted preventive measures to manage the spread of the epidemic. We will also analyze how these controls affect the reproduction number, demonstrating that while adequate controls may increase the reproduction number, they still lead to a decrease in disease transmission and the number of individuals in quarantine. Finally, in section 4, we will present numerical simulations that confirm the effectiveness of the optimal control strategy.

2. Model Formulation

First, we examine Equation (1.1), where the parameters are defined based on the data presented in Table 1, as referenced in [1]. We note that the overall stability of both the disease-free and endemic states is analyzed and discussed in [1]. The requirement for the above system to be biologically meaningful is that the relations in Equation (1.1) under

TABLE 1. Detailing the parameters applied in Equation (1.1).

parameters	physical explanation
Λ	Employment rate among susceptibles
a	Infection transmission rate
b	Recruitment rate among healthy individuals
c	Transmission rate among healthy people
d	Natural mortality rate
μ	Disease related death rate
α	Quarantined people infection rate
β	Quarantined cure rate
γ	Infection transmission rate

initial values $S(0), H(0), I(0), Q(0)$ which are all positive. For this purpose, we refer to the following theorem:

Theorem 2.1. *[1] The set* $\Gamma = \{(S, H, I, Q) \in R^4_+ : S + H + I + Q \leq (\Lambda + b)/A_1\}$ *is positively invariant for Equation (1.1) with the initial values* $S(0) \geq 0$, $H(0) \geq 0$, $I(0) \geq 0$, *and* $Q(0) \geq 0$.

When the population is infection-free ($I = Q = 0$), the system's equilibrium, denoted by E^0, is the disease-free equilibrium (DFE). Setting $I = Q = 0$ and solving for $H(t)$ and $S(t)$ yields:

$$E^0(S^0, H^0, I^0, Q^0) = (S^0, H^0, 0, 0) = \left(\frac{\Lambda}{A_1}, \frac{b}{A_1}, 0, 0\right),$$

To determine the behavior of the dynamical system, we calculate the basic reproduction number, R_0 [11]. Considering the infected compartments $Y = (I, Q)^T$ in Equation (1.1), R_0 can be obtained by setting:

$$A_1 = d + \mu, \quad A_2 = d + \mu + \gamma + \beta, \quad A_3 = d + \mu + \alpha. \tag{2.1}$$

Then

$$\frac{dY}{dt} = \begin{pmatrix} \frac{dI}{dt} \\ \frac{dQ}{dt} \end{pmatrix} = \begin{pmatrix} aS(t)I(t) + cH(t)I(t) - A_2 I(t) + \alpha Q(t) \\ \gamma I(t) - A_3 Q(t) \end{pmatrix}$$
$$= \underbrace{\begin{pmatrix} aS + cH & 0 \\ 0 & 0 \end{pmatrix}}_{:=F} \begin{pmatrix} I(t) \\ Q(t) \end{pmatrix} - \underbrace{\begin{pmatrix} A_2 & -\alpha \\ -\gamma & A_3 \end{pmatrix}}_{:=V} \begin{pmatrix} I(t) \\ Q(t) \end{pmatrix}.$$

The reproduction matrix for the proposed Disease-Free Equilibrium (DFE) is defined as follows:

$$FV^{-1} = \frac{1}{A_2 A_3 - \gamma\alpha} \times \begin{pmatrix} (\frac{a\Lambda + cb}{A_1})A_3 & \alpha(\frac{a\Lambda + cb}{A_1}) \\ 0 & 0 \end{pmatrix}.$$

The basic reproduction number R_0 is given by the spectral radius of the relevant matrix.

$$R_0 = max\left\{|e| : e \text{ be an eigenvalue of } \ FV^{-1}\right\} = \frac{(a\Lambda + cb)A_3}{A_1(A_2A_3 - \gamma\alpha)}. \tag{2.2}$$

Theorem 2.2. *[1] The critical point DFE in Equation (1.1) is locally asymptotically stable, provided that the threshold quantity $R_0 < 1$, and*

$$C_1 : \frac{bc + a\Lambda}{A_1} < A_2;$$

Otherwise, the critical point DFE for the dynamical system described in Equation (1.1) will be unstable.

Now, let $X(t) = (S(t), H(t))^T \in \mathbb{R}^2_+$ and $Y(t) = (I(t), Q(t))^T \in \mathbb{R}^2_+$ represent the susceptible/healthy and infected/quarantined populations, respectively. Equation (1.1) can be decomposed as:

$$\frac{dX}{dt} = F(X, Y), \qquad \frac{dY}{dt} = U(X, Y).$$

Also assume that

$$B = \begin{pmatrix} aS^0 + cH^0 - A_2 & \alpha \\ \gamma & -A_3 \end{pmatrix}, \quad U^*(X, Y) = \begin{pmatrix} (aI + cI)(S^0 + H^0) + (aI + cI)(S + H) \\ 0 \end{pmatrix}.$$

Lemma 2.3. *[1] If $R_0 < 1$, the critical point $E^0 = (X^0, 0)$ is asymptotically globally stable for the dynamic model (1.1) under the following conditions:*

C1: *If $X^{'} = F(X, 0)$, then X^0 is globally asymptotically stable.*
C2: *The function $U(X, Y)$ is defined as $BY - U^*(X, Y)$, wherever $U^*(X, Y) \geq 0$ for $(X, Y) \in \Gamma$.*

The endemic equilibrium $E^* = (S^*, H^*, I^*, Q^*)$ of Equation (1.1), where $I^* \neq 0$, satisfies:

$$S^* = \frac{\Lambda}{aI^* + A_1}, \ H^* = \frac{b + \beta I^*}{cI^* + A_1}, \ I^* = \frac{\alpha Q^*}{A_2 - aS^* - cH^*}, \ Q^* = \frac{\gamma I^*}{A_3}. \tag{2.3}$$

By substituting H^*, S^*, and Q^* into I^* of Equation (2.3), we derive at the quadratic equation:

$$f(I^*) = x_1 {I^*}^2 + x_2 I^* + x_3, \tag{2.4}$$

where $x_1 = ac$, $x_2 = (a+c)A_1 - c(a\Lambda + \beta)$, and $x_3 = A_1^2(1 - R_0)$. Since $a, c > 0$, $x_1 > 0$. The following theorem, derived in [1], characterizes the number of endemic equilibria of the dynamical system (1.1) based on the coefficients of Equation (2.4).

Theorem 2.4. *[1] For Equation (1.1):*

1) $x_3 < 0 \Leftrightarrow R_0 > 1$. *In this case, Equation (1.1) possesses a unique endemic equilibrium.*
2) *If* $x_2 < 0$ *and either* $x_3 = 0$ *or* $x_2^2 - 4x_1x_3 = 0$, *then Equation (1.1) possesses a unique endemic equilibrium.*
3) *If* $x_3 > 0$, $x_2 < 0$, *and* $x_2^2 - 4x_1x_3 > 0$, *then Equation (1.1) possesses two endemic equilibria.*
4) *In other conditions, Equation (1.1) does not have an endemic equilibrium.*

The third case outlined in Theorem 2.4 illustrates backward bifurcation, where both the disease-free equilibrium (DFE) and an endemic equilibrium are locally asymptotically stable when $R_0 < 1$. To analyze this bifurcation, we find the critical value R_c of R_0 by setting the discriminant $x_2^2 - 4x_1x_3$ equal to zero:

$$R_c = 1 - \frac{x_2^2}{4ac{A_1}^2}.$$

Backward bifurcation occurs when $x_2^2 - 4x_1x_3 > 0$ or when $1 > R_0 > R_c$. This phenomenon is significant in epidemiology because it requires $R_0 < 1$ for the backward bifurcation event to take place. However, although this condition is necessary, it is not sufficient for the elimination of a disease. In this context, the disappearance of the disease is directly influenced by the initial conditions of the state variables. Interestingly, disease control under backward bifurcation can still be observed even when $R_0 > 1$, depending on the initial size of the sub-population.

Lemma 2.5. *[1] System (1.1) exhibits backward bifurcation if* $x_3 > 0$, $x_2 < 0$, *and* $x_2^2 - 4x_1x_3 > 0$, *along with* $R_c < R_0 < 1$. *Furthermore, if* $R_0 = 1$, *then Equation (1.1) will endure a backward bifurcation if and only if* $x_2 < 0$.

The global stability of the endemic equilibrium E^* of Equation (1.1) is determined by the threshold parameter R_0.

Theorem 2.6. *[1] The endemic equilibrium* E^* *Equation (1.1) is globally asymptotically stable if* $R_0 > 1$.

3. Optimal Control

By mid-November 2020, several COVID-19 vaccines had entered the final stages of development in countries such as China, the United States, and Iran, among others. Therefore, we propose the following strategies, which include control variables, to represent interventions aimed at curbing the spread of the virus. The controls $u(t)$, $v(t)$, and $w(t)$ are defined over the interval $t \in [0, T]$. The first control, $u(t)$, focuses on reducing the transmission of the disease from susceptible individuals to infected individuals through public and personal protection measures. The second control, $v(t)$, involves vaccination strategies to decrease transmission within the healthy population. The third control, $w(t)$, pertains to quarantine management and aims to lower the transmission rate among those in quarantine.

As a result, the controlled system is described as follows:

$$\begin{cases} \dfrac{dS(t)}{dt} = \Lambda - a(1-u(t))S(t)I(t) - A_1S(t), \\ \dfrac{dH(t)}{dt} = b - c(1-v(t))H(t)I(t) + \beta I(t) - A_1H(t), \\ \dfrac{dI(t)}{dt} = a(1-u(t))S(t)I(t) + c(1-v(t))H(t)I(t) + \alpha Q(t) - A_2I(t), \\ \dfrac{dQ(t)}{dt} = \gamma(1+w(t))I(t) - A_3Q(t). \end{cases} \tag{3.1}$$

First, we examine the effect of the basic reproductive number under both controlled and uncontrolled conditions in a disease-free environment. Our focus is on assessing the potential state of the system with control (3.1) and understanding its equilibrium nature. We assume that there is no infection in the population, or, equivalently, that we have $I = Q = 0$. This corresponding state is referred to as the Disease-Free Equilibrium (DFE) in the controlled state. The infected group includes the variables I and Q, which we can define as follows:

$$Y = (I(t), (Q(t))^T,$$

In the system described by Equation (3.1), to find the equilibrium E_c^0, we set $I = Q = 0$. By solving the system's differential equations for $H(t)$ and $S(t)$, we obtain the necessary results:

$$\begin{cases} \Lambda - A_1 S(t) = 0 \\ b - A_1 H(t) = 0 \end{cases} \equiv \begin{cases} A_1 S(t) = \Lambda \\ A_1 H(t) = b \end{cases} \equiv \begin{cases} S(t) = \dfrac{\Lambda}{A_1}, \\ H(t) = \dfrac{b}{A_1}, \end{cases} \tag{3.2}$$

Therefore, the critical point for the system under control is represented as

$$E_c^0(S^0, H^0, I^0, Q^0) = (S^0, H^0, 0, 0) = \left(\frac{\Lambda}{A_1}, \frac{b}{A_1}, 0, 0\right).$$

The basic generator number (R_{0c}) in the controlled state plays a critical role in the overall behavior of the system described in Equation (1.1). To understand this better, we need to calculate the spectral radius of the matrix FV^{-1} [11]. In this context, let's consider Equation (2.1), which addresses the contaminated group in the system described in Equation (3.1). The contaminated group, denoted as $Y = (I, Q)^T$, is given by:

$$\begin{aligned} \frac{dY}{dt} &= \begin{pmatrix} \dfrac{dI}{dt} \\ \dfrac{dQ}{dt} \end{pmatrix} = \begin{pmatrix} a(1-u(t))S(t)I(t) + c(1-v(t))H(t)I(t) - A_2 I(t) + \alpha Q(t) \\ \gamma(1+w(t))I(t) - A_3 Q(t) \end{pmatrix} \\ &= \begin{pmatrix} (a(1-u(t))S(t) + c(1-v(t))H(t))I(t) \\ 0 \end{pmatrix} - \begin{pmatrix} A_2 I(t) - \alpha Q(t) \\ -\gamma(1+w(t))I(t) + A_3 Q(t) \end{pmatrix}. \end{aligned}$$

so

$$\begin{aligned} \frac{dY}{dt} &= \begin{pmatrix} (a(1-u(t))S(t) + c(1-v(t))H(t))I(t) \\ 0 \end{pmatrix} - \begin{pmatrix} A_2 I(t) - \alpha Q(t) \\ -\gamma(1+w(t))I(t) + A_3 Q(t) \end{pmatrix} \\ &= \begin{pmatrix} a(1-u(t))S(t) + c(1-v(t))H(t) & 0 \\ 0 & 0 \end{pmatrix} \begin{pmatrix} I(t) \\ Q(t) \end{pmatrix} - \begin{pmatrix} A_2 & -\alpha \\ -\gamma(1+w(t)) & A_3 \end{pmatrix} \begin{pmatrix} I(t) \\ Q(t) \end{pmatrix}. \end{aligned} \tag{3.3}$$

The Jacobians of the above matrices are, in order, provided with:

$$F = \begin{pmatrix} a(1-u(t))S^0 + c(1-v(t))H^0 & 0 \\ 0 & 0 \end{pmatrix}, \qquad V = \begin{pmatrix} A_2 & -\alpha \\ -\gamma(1+w(t)) & A_3 \end{pmatrix}.$$

Computation is applied to find out the matrix inverse of V, we get

$$V^{-1} = \frac{1}{A_2 A_3 - \gamma\alpha(1+w(t))} \times \begin{pmatrix} A_3 & \alpha \\ \gamma(1+w(t)) & A_2 \end{pmatrix}.$$

The matrix of the proposed model (DFE) in the controlled state is as follows:

$$FV^{-1} = \begin{pmatrix} \left(\dfrac{a(1-u(t))\Lambda + c(1-v(t))b}{A_1\left(A_2 A_3 - \gamma\alpha(1+w(t))\right)}\right) A_3 & \alpha\left(\dfrac{a(1-u(t))\Lambda + c(1-v(t))b}{A_1\left(A_2 A_3 - \gamma\alpha(1+w(t))\right)}\right) \\ 0 \end{pmatrix}.$$

The threshold parameter R_{0c} is provided by the spectral radius of this matrix $\left(FV^{-1}\right)$, hence

$$R_{0c} = \left(FV^{-1}\right) = max\left\{|e| : e \text{ be an eigenvalue of } FV^{-1}\right\} = \frac{(a\Lambda(1-u(t)) + cb(1-v(t)))A_3}{A_1\left(A_2 A_3 - \gamma\alpha(1+w(t))\right)}. \tag{3.4}$$

At this stage, the objective function needs to be minimized.

$$J(u, v, w) = I(T) + Q(T) + \int_0^T \left[I(t) + Q(t) + \frac{1}{2}\left(Au^2(t) + Bv^2(t) + Gw^2(t)\right)\right] dt, \tag{3.5}$$

Where T denotes the terminal time, and the cost coefficients are represented by $A > 0$, $B > 0$, and $G > 0$. These coefficients are chosen at time t to measure the relative significance of $u(t)$, $v(t)$, and $w(t)$. Next, we identify u^*, v^*, and w^* that minimize the cost functional:

$$J(u^*, v^*, w^*) = \min_{u,v,w \in U} J(u, v, w), \tag{3.6}$$

where U includes the set of introduced controls with specified bounds,

$$U = \left\{ \begin{array}{c} u, v, w \mid 0 \le u_{\min} \le u(t) \le u_{\max} \le 1,\ 0 \le v_{\min} \le v(t) \le v_{\max} \le 1, \\ \text{and} \quad 0 \le w_{\min} \le w(t) \le w_{\max} \le 1, \quad t \in [0, T] \end{array} \right\}, \tag{3.7}$$

The cost function J quantifies the number of infected ($I(T)$) and quarantined ($Q(T)$) individuals at time T, along with the cumulative number of individuals in these compartments and the total cost of the quarantine policy up to time T through the integral part of the function. Thus, minimizing J in Equation (3.6) reduces disease spread and optimizes quarantine policies by minimizing the number of infected and quarantined individuals both at the final time and throughout the simulation, while also considering the costs of control measures.

It should be noted that the personal protection control, i.e., ($u(t)$), the vaccination control, i.e., ($v(t)$), and the quarantine control, i.e., ($w(t)$) are introduced at time $t \in [0, T]$, and the control space U is convex and closed to ensure the existence of optimal control. Each of these controls is also bounded between 0 and 1. Personal protection ($u(t)$) encompasses measures like mask-wearing, glove use, and social distancing, ranging from no protection (0) to full compliance (1), with $0 \le u_{min} \le u(t) \le u_{max} \le 1$ defining the minimum and maximum protection levels. Similarly, vaccination control ($v(t)$) represents the vaccination strategy to increase population immunity, from no vaccination (0) to full coverage (1), bounded by $0 \le v_{min} \le v(t) \le v_{max} \le 1$, representing minimum effort and maximum capacity; and finally, quarantine control ($w(t)$) manages quarantine measures to reduce transmission, ranging from no quarantine (0) to fully effective quarantine (1), with $0 \le w_{min} \le w(t) \le w_{max} \le 1$ defining the range of effectiveness. These constraints are essential for the optimal control problem.

First, the existence of solutions for the system in Equation (3.1) is proven, followed by the establishment of the existence of an optimal control [6].

Theorem 3.1. *We prove for the controlled system (3.1), optimal controls $(u^*, v^*, w^*) \in U$ that there exist controls that satisfy the following relation:*

$$J(u^*, v^*, w^*) \ \ is \ \ defined \ \ as \ \ \min_{u,v,w \in U} J(u, v, w),$$

i.e., minimize the cost functional.

Proof. Using a result from [6], the existence of an optimal control can be demonstrated by verifying the following steps:

Step 1: We will show that the controls set u, v and w also the state variables S, H, I, and Q are not empty. Using a simplified model, we will examine the nonemptiness of state and control variables [2].

Suppose $X_i' = f_{X_i}(t; X_1, X_2, X_3, X_4)$ where $(X_1, X_2, X_3, X_4) = (S, H, I, Q)$ for $i = 1, ..., 4$ where X_1,..., and X_4 correspond to the right-hand side of Equation (3.1). Since all parameters are constant and assuming that u, v and w are constant Given that X_1, ..., and X_4 are continuous, then f_S, f_H, f_I, and f_Q are also continuous. Furthermore, $\frac{\partial f_{X_i}}{\partial_{X_i}}$ for $i = 1, ..., 4$, i.e., all partial derivatives are continuous functions. So, there is a unique solution (S, H, I, Q) satisfying the initial conditions. Thus, the non-infinity of the control sets and state variables is satisfied.

Step 2: We demonstrate that the cost function $J(u, v, w)$ is convex in U. Let $u, v \in U$ and $\lambda \in [0, 1]$. Since U is a convex set, $\lambda u + (1 - \lambda)v \in U$. The convexity of J then follows directly from the convexity of its constituent terms.

Step 3: The control space U is measurable. Indeed

$$0 \le u_{min} \le u(t) \le u_{max} \le 1, \quad 0 \le v_{min} \le v(t) \le v_{max} \le 1, \quad 0 \le w_{min} \le w(t) \le w_{max} \le 1, \ t \in [0, T],$$

The right-hand side of Equation (3.1), with a set of control variables and bounded state variables, are continuous and can be expressed as a linear function of the controls that depend on (t) and the state variables. Therefore, it is convex and closed under the stated conditions.

Step 4: The expression within the integral of the function J is convex on U.
Step 5: Thus, it remains to show the existence of positive constants $\xi_1, \xi_2, \xi_3, \xi_4$ and ξ so that

$$I(t) + Q(t) + \frac{1}{2}\left(Au^2(t) + Bv^2(t) + Gw^2(t)\right) \geq \xi_1 + \xi_2|u|^{\xi} + \xi_3|v|^{\xi} + \xi_4|w|^{\xi}.$$

Given that the state variables are limited within certain bounds, we define $\xi_1 = \inf_{t\in[0,T]}(I(t)+Q(t))$, $\xi_2 = \frac{A}{2}$, $\xi_3 = \frac{B}{2}$, $\xi_4 = \frac{G}{2}$, and $\xi = 2$. Then, the inequality holds. According to [6], we conclude that an optimal control exists. □

We use the Pontryagin maximum [10] principle to obtain the necessary conditions for optimal control over the following Hamiltonian equation $\mathcal{H}(t)$ at time t:

$$\mathcal{H}(t) = I(t) + Q(t) + \frac{1}{2}\left(Au^2(t) + Bv^2(t) + Gw^2(t)\right) + \sum_{i=1}^{4}\lambda_i(t)f_i(S, H, I, Q), \tag{3.8}$$

Here, f_i denotes the right side of the equations corresponding to the i^{th} state variable

Theorem 3.2. *Let the solutions S^*, H^*, I^*, and Q^* of Equation (3.1) and (u^*, v^*, w^*) be given. Then, there exist adjoint state variables λ_1, λ_2, λ_3, and λ_4 satisfying*

$$\begin{aligned}
\lambda_1' &= \lambda_1\left((1-u(t))aI(t) + A_1\right) - \lambda_3\left((1-u(t))aI(t)\right),\\
\lambda_2' &= \lambda_2\left((1-v(t))cI(t) + A_1\right) - \lambda_3((1-v(t))cI(t)),\\
\lambda_3' &= -1 + \lambda_1\left((1-u(t))\,aS(t)\right) - \lambda_2\left(-((1-v(t))cH(t) + \beta) - \lambda_3((1-u(t))aS(t)\right.\\
&\quad + \qquad\qquad\qquad\qquad\qquad\qquad\qquad\qquad (1-v(t))cH(t) - A_2) - \lambda_4(1+w(t))\\
\lambda_4' &= -1 - \lambda_3\alpha + \lambda_4 A_3.
\end{aligned}$$

Under the transverse conditions in control theory at the final time T : $\lambda_1(T) = 0$, $\lambda_2(T) = 0$, $\lambda_3(T) = -1$, and $\lambda_4(T) = -1$. Moreover, u^*, v^*, and w^* at time t are determined as follows:

$$u^* = \min\left(1, \max\left(0, \frac{(\lambda_3 - \lambda_1)}{A}\left(aS(t)I(t)\right)\right)\right), \tag{3.9}$$

$$v^* = \min\left(1, \max\left(0, \frac{(\lambda_3 - \lambda_2)}{B}cH(t)I(t)\right)\right), \tag{3.10}$$

$$w^* = \min\left(1, \max\left(0, -\frac{\lambda_4}{G}\gamma I(t)\right)\right). \tag{3.11}$$

Proof. Consider the time-dependent Hamiltonian function $\mathcal{H}(t)$ with

$$\begin{aligned}
f_1(S, H, I, Q,) &= \Lambda - a(1-u(t))S(t)I(t) - A_1S(t),\\
f_2(S, H, I, Q,) &= b - c(1-v(t))H(t)I(t) + \beta I(t) - A_1H(t),\\
f_3(S, H, I, Q,) &= a(1-u(t))S(t)I(t) + c(1-v(t))H(t)I(t) + \alpha Q(t) - A_2I(t),\\
f_4(S, H, I, Q,) &= \gamma(1+w(t))I(t) - A_3Q(t).
\end{aligned}$$

By applying Pontryagin's maximum principle over $t \in [0, T]$, one can obtain the adjoint equations together with the transversality conditions. [8, 10], such that

$$\begin{aligned}
\lambda_1' &= -\frac{\partial \mathcal{H}(t)}{\partial S} = \lambda_1\left((1-u(t))aI(t) + A_1\right) - \lambda_3\left((1-u(t))aI(t)\right),\\
\lambda_2' &= -\frac{\partial \mathcal{H}(t)}{\partial H} = \lambda_2\left((1-v(t))cI(t) + A_1\right) - \lambda_3((1-v(t))cI(t)),\\
\lambda_3' &= -\frac{\partial \mathcal{H}(t)}{\partial I} = -1 + \lambda_1\left((1-u(t))aS(t)\right) - \lambda_2\left(-((1-v(t))cH(t) + \beta\right)\\
&\quad - \lambda_3\Big((1-u(t))aS(t) + (1-v(t))cH(t) - A_2\Big) - \lambda_4(1+w(t))\gamma,\\
\lambda_4' &= -\frac{\partial \mathcal{H}(t)}{\partial Q} = -1 - \lambda_3\alpha + \lambda_4 A_3.
\end{aligned}$$

u^*, v^*, and w^* for $t \in [0, T]$, are obtained by solving the optimality condition.

$$\begin{aligned}
-\frac{\partial \mathcal{H}(t)}{\partial u} &= -Au(t) + (\lambda_3 - \lambda_1)(aS(t)I(t)) = 0,\\
-\frac{\partial \mathcal{H}(t)}{\partial v} &= -Bv(t) + (\lambda_3 - \lambda_2)cH(t)I(t)) = 0,\\
-\frac{\partial \mathcal{H}(t)}{\partial w} &= -Gw(t) - \lambda_4\gamma I(t) = 0.
\end{aligned}$$

so,

$$u(t) = \frac{(\lambda_3 - \lambda_1)}{A}aS(t)I(t), \quad v(t) = \frac{(\lambda_3 - \lambda_2)}{B}cH(t)I(t), \quad w(t) = -\frac{\lambda_4}{G}\gamma I(t).$$

Using the bounds on the controls in U, it is straightforward to catch u^*, v^*, and w^* as presented in Equations (3.9), (3.10), and (3.11), respectively, in the form of Equation (1.1). □

We end this section by notifying that the adjoint equations are derived from the negative partial derivative of the Hamiltonian for each state variable. The adjoint variables λ_i represent the sensitivity of the cost function $J(u(t), v(t), w(t))$ to infinitesimal changes in the state variables at time t, reflecting the instantaneous cost and the interaction of state variables. More specifically, $\lambda_1, \lambda_2, \lambda_3$, and λ_4 reflect, respectively, the impact of changes in susceptible individuals $S(t)$, healthy individuals $H(t)$, infected individuals $I(t)$, and quarantined individuals $Q(t)$ on the marginal cost.

Optimal controls, obtained through Hamiltonian optimization, depend on the state and adjoint variables. Critically, $u^*(t)$, $v^*(t)$, and $w^*(t)$ are determined by differences between the λ_is, implying that control decisions (personal protection, vaccination, quarantine) are based on the "relative value" of reducing or increasing each state variables $S(t)$, $H(t)$, $I(t)$, and $Q(t)$ to minimize the total cost. For example, in the equation for $u^*(t)$ (personal protection), the term $(\lambda_3 - \lambda_1)$ appears, indicating that the optimal level of personal protection depends on the difference between the adjoint variables for infected and susceptible individuals. If λ_3 is significantly less than λ_1, reducing $I(t)$ is more valuable, incentivizing increased personal protection to reduce the flow from $S(t)$ to $I(t)$. This represents dynamic feedback within the optimal control system, enforced via the adjoint variables.

4. Numerical Results, Discussion and Conclusion

This section provides numerical simulation of the behavior of the controlled COVID-19 model (3.1). The simulation evaluates the impact of the effectiveness controls on the initial populations $S(0)$, $H(0)$, $I(0)$, and $Q(0)$ up to time T. The parameter values are set up as detailed in Table 2; and they are as same as those of uncontrolled model in [1] and they are based on the World Health Organization (WHO) statistics cited in [8, 12]. This enables us to compare our results with those of the uncontrolled model in [1].

TABLE 2. Detailing the parameters applied in the system Equation (1.1).

Parameters	Physical reasoning	scalar values (In units of 1000 people)
$S(t)$	Susceptible individuals	1000
$H(t)$	Healthy individuals	790
$I(t)$	Infected individuals	170
$Q(t)$	People in quarantine	450
Λ	Employment rate among susceptibles	0/0043217
a	Infection transmission rate	0/125
b	Employment rate among healthy individuals	0/535
c	Permeation rate among healthy people	0/0056
d	Natural mortality rate	0/002
μ	Disease related death rate	0/0008
α	Quarantined people's infection rate	0/029
β	Quarantined cure rate	0/35
γ	Infection transmission rate	0/025

The disease-free equilibrium (DFE) of uncotrolled model (1.1) is $E^0 \approx (1.5472, 191.071, 0, 0)$, with eigenvalues $e_1 = e_2 = -0.0028$, $e_3 = 0.8860$, $e_4 = -0.02887$, and $R_0 \approx 3.559 > 1$. Theorem 2.2 indicates that E_0 is unstable. Furthermore, according to Theorems 2.4 (part 1) and 2.6, the uncontorolled model (1.1) has a unique endemic equilibrium, $E^* \approx (0.00047885, 63.3824, 72.3538, 56.8819)$ which is globally asymptotically stable.

In what follows, the contorolled model (3.1) is solved by iteratively updating initial guesses for control variables $u(t)$ (vaccination rate), $v(t)$ (quarantine), and $w(t)$ (awareness campaigns). Simulations show that the controls are effective in reducing disease outbreaks and quarantine numbers, but their impact on the controlled basic reproductive number R_{0c} is limited. It should be noted that, in Equation (3.1), DFE singularity persists and remains unstable; however, due to the time dependence of the controls, the endemic singularity might not exist.

TABLE 3. Percentage reduction in infected and quarantined people in controlled and uncontrolled conditions.

The total amount after 100 days	uncontrolled	controlled	Percent decrease
$I(t)$	975	634.7	65.09
$Q(t)$	830.9	544.8	65.56

The critical basic reproduction number, $R_c = -115.232$, is meaningless, indicating that backward bifurcation does not occur. The global stability of E^* necessitates the implementation of effective control measures to dampen the infection rate more rapidly and effectively, as discussed below.

To address differing scales between control and state functions, cost constants in Equation (3.5) are set to A=B=G = 1000. These weights correspond to the costs of personal protection ($u(t)$), vaccination ($v(t)$), and quarantine ($w(t)$). This choice follows two key points: first, the model assigns equal relative importance to all three control strategies; second, it emphasizes the significant cost of implementing these controls, aligning to minimize disease impact and control costs. The initial values for both controlled and uncontrolled models are chosen as S(0) = 1000, H(0) = 790, I(0) = 170, and Q(0) = 450. The objective is to minimize costs, balancing the disease's impact (infections, hospitalizations) and control expenses (quarantine, vaccination).

In the controlled model with feedbacks $(u(t), v(t), w(t))$, the control effect appears only when the infected population becomes large; therefore, the initial growth of the disease is not suppressed, and the system still approaches an endemic state. Numerical analysis further indicates that, under this feedback structure, the effective basic reproduction number can even be larger than in the uncontrolled case, due to nonlinear interactions that increase the effective transmission coefficients at equilibrium. In contrast, an optimally designed control strategy that reduces transmission from the

beginning can guide the epidemic trajectory toward faster suppression rather than stabilization at endemic levels. Even with minimal intervention, spontaneous actions such as handwashing or limited vaccination/quarantine may occur, which implies that u_{min}, v_{min}, and w_{min} are close to zero, but not necessarily zero. u_{max}, v_{max}, and w_{max} represent achievable maximum levels, influenced by health system capacity, public acceptance, and resource availability. While ideally 1, practical limitations may result in values less than 1, reflecting challenges in achieving perfect personal protection, full vaccination, or complete quarantine.

4.1. **Strategy A: Personal protection strategy.** The control strategy $u(t)$ aims to reduce transmission of the disease from susceptible individuals $S(t)$ to infected individuals $I(t)$. Figure 2 shows the infected group $I(t)$ over 0 to 100 days with an initial value of $I(0) = 170$ in uncontrolled and controlled cases, for different values of β (the recovery rate in quarantine) of $0.1, 0.35, 0.7$, and 1. Figure 2 displays that at the beginning of the epidemic, the population of an infected group, $I(t)$, increased approximately 2000, and Figure 3 shows the decline of the susceptible people, $S(t)$. (At the beginning of the pandemic, a great portion of the population was "susceptible" to infection, meaning they were at risk of contracting it. Over time, as the disease spreads, susceptible individuals become infected and are eliminated from the susceptible population. The decline in this graph over time represents the same process as susceptible individuals reduce the population of this group upon contracting the epidemic. As the infected case count and quarantined individuals increase, we will simultaneously see a decline in the number of susceptible individuals as they are transmitted to other groups). This rapid population growth is a key feature of infectious diseases like COVID-19, which increases rapidly when conditions are favorable for transmission. This increase is also a result of the lack of adherence to health protocols such as handwashing, mask use, contact with infected individuals, public education strategies, etc. In an uncontrolled state, this population will decrease by half its initial increase over a given period, partly due to the above and vaccination. While with the implementation of personal protection controls and vaccination, the initial increase is almost half of the rise in the uncontrolled population, and within a hundred days, with the implementation of personal protection principles (wearing masks, frequent hand washing, social distancing, etc.), this population has decreased significantly again, indicating the effectiveness of the relevant controls. By performing calculations and comparing the graphs for different values of β, we conclude that as the amount β increases, the infected people and infection transmission decrease. Table 3 shows how personal protection measures and contact reduction affect the susceptible individuals $S(t)$ before and after implementation. Over one hundred days, in infected individuals, there was a decrease of about 65.09 in both the controlled and uncontrolled cases. In general, the rise in infected individuals from 170 is due to the disease transmission dynamics within the mathematical model. This dynamic is influenced by the transmission rate between susceptible and healthy populations, as well as the absence of effective epidemic control measures, bringing about an increase in the number of infections. This increase is a natural consequence of the transmission of the disease within a population that has not yet achieved herd immunity, and control measures are not fully observed. Key preventive measures, including social distancing, mask use, and hygiene practices, are crucial to prevent virus transmission. Awareness programs play a key role in educating citizens about the severity of COVID-19 and encouraging behaviors such as frequent hand washing and mask use.

4.2. **Strategy B: Vaccination strategy.** The control strategy $v(t)$ focuses on reducing the transmission of the disease from healthy individuals $H(t)$ and susceptible individuals $S(t)$. Figures 3 and 4 show the susceptible and healthy groups with initial values $S(0) = 1000$ and $H(0) = 790$ throughout 0 to 100 days in the ermanent, and over time, the body's immune response decreases, so the recovered person becomes reinfected and is transferred to the susceptible group. As is known from $COVID - 19$, immunity from natural infection or vaccination may not be permanent and may decrease over time. Also, at the onset of the disease, the number of recovered and healthy people may increase, but over time, if the rate of waning immunity increases, the number of people in this group may decrease, or if a new wave of the disease occurs with new strains, previously resistant people may become susceptible again. In the uncontrolled state, the population of the healthy group $H(t)$ initially decreases and at some point in time becomes less than the population of the healthy group in the controlled state, which indicates the positive effect of control $v(t)$, i.e., the vaccination control has a positive effect on the increase in the healthy population in the controlled state. In Figures 3 and 4, with the change in β, there is almost no change in the graph. In other words, the parameter β does not have a large effect on the increase in the population of the healthy and susceptible group. While controlling

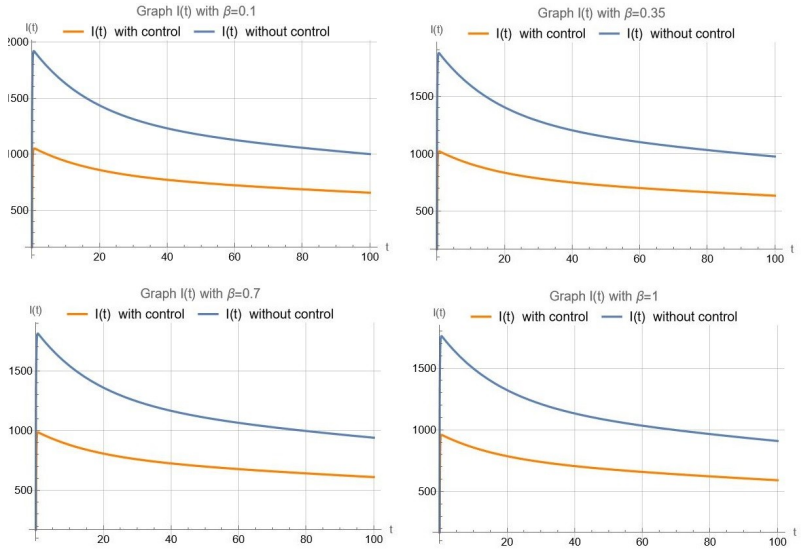

FIGURE 2. Comparative graph of $I(t)$ in terms of parameter β with different values in uncontrolled and controlled systems.

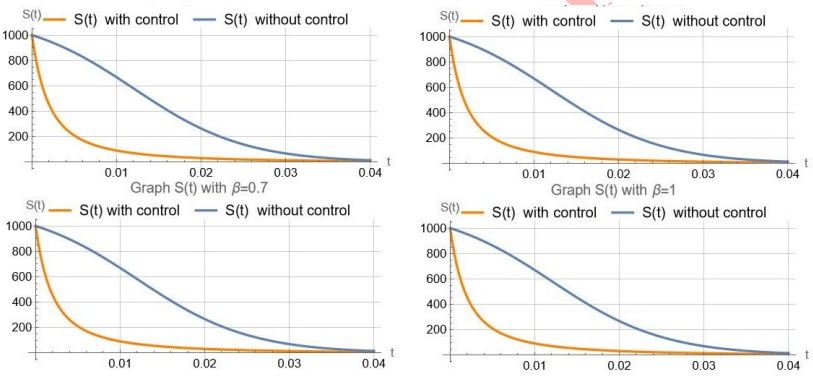

FIGURE 3. Comparison chart of $S(t)$ in terms of parameter β with different values in uncontrolled and controlled systems.

$v(t)$ has a positive effect compared to the uncontrolled state. This strategy can significantly decrease the number of infections and thus alleviate the impact of the disease on the healthcare system. When controlling $v(t)$ is applied, in addition to increasing the population of the healthy group, it also reduces the probability of disease through a vaccination strategy to increase population immunity and health awareness campaigns to encourage vaccination. The statistics in Table 3 are the results related to the effect of vaccination on infected and quarantined individuals.

4.3. **Strategy C: Quarantine strategy.** The control strategy $w(t)$ focuses on the quarantine management of infected individuals $I(t)$ and the reduction of the transmission rate among the individuals in quarantine, which includes strategies for quarantining infected individuals and managing contacts and tracing at-risk individuals. Figure 5 shows the quarantine group in the pre- and post-control states, showing the effects of quarantine management measures on the number of individuals in this group, as well as their influence on lowering the number of infected individuals and reducing transmission. This group is plotted over 0 to 100 days with an initial value of $Q(0) = 450$ in the uncontrolled and controlled state for different values of β (the recovery rate in quarantine) of 0.1, 0.35, 0.7, and 1. The plot

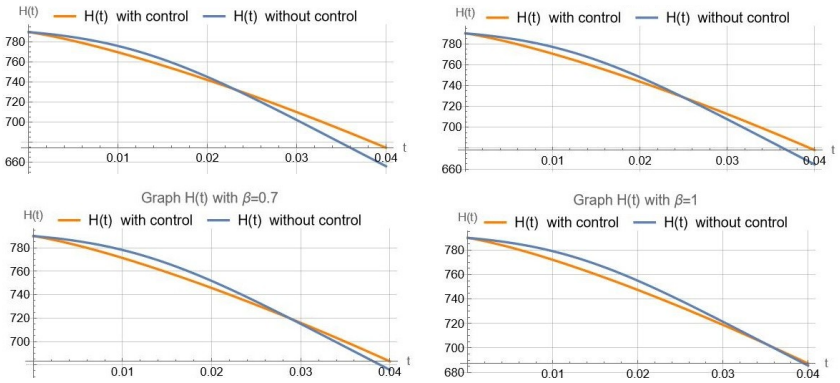

FIGURE 4. Comparison chart of $H(t)$ in terms of parameter β with different values in uncontrolled and controlled systems.

shows that at the beginning of the outbreak, the population of the quarantine group $Q(t)$ (almost the first 40 days) gradually increased with a slightly steep slope for different values of β. This increase is due to a lack of awareness and non-compliance with health protocols, increased infected individuals, and re-infection of quarantined individuals. The decrease in the quarantine population during the remaining period is due to the discharge of those who have recovered due to compliance with guidelines and protocols. While the implementation of quarantine control and compliance with protocols and vaccination at the beginning of the outbreak had a more minor increase than the uncontrolled cases, here, it is also shown that with the rise in the value of β, the population of this group decreases significantly. Over one hundred days, a decrease of about 65.56 is observed in both controlled and uncontrolled cases, indicating a positive effect of quarantine control $w(t)$, which includes measures such as hospitalization, provision of medicine, and other treatments such as quarantine, which reduces the quarantine population and subsequently reduces the number of infected people and accelerates their recovery. Table 3 shows the results related to this strategy. In short, the increase in the population of quarantined people is a function of the rise in the infected population due to the outbreak and quarantine policies. It is a direct result of the lack of control over the outbreak. As the number of infected individuals grows, so does the need for isolation to control the epidemic, resulting in a rising trend. Finally, in Figure 6, we plot R_0 and R_{0c} against different parameters involved in Equations (1.1) and (3.1) under consideration. This Figure demonstrates that, although the control achieved in this study increases the reproduction number, as shown in the results, it ultimately reduces the number of sick individuals and effectively controls the disease.

The findings from our study can be effectively summarized by highlighting the significant impact of optimal control strategies on mitigating the spread of the coronavirus, as demonstrated through a mathematical model. The application of these controls demonstrably reduces disease transmission and effectively manages the propagation of infectious diseases within the modeled population. Specifically, the anticipated and desired outcomes were successfully achieved through the strategic implementation of three key policy interventions: personal protection measures, a comprehensive vaccination program, and the imposition of quarantine protocols. These policies are mathematically represented and analyzed through control variables, denoted respectively as $u(t)$ for personal protection, $v(t)$ for vaccination efforts, and $w(t)$ for quarantine measures. The optimization of these control variables was specifically geared towards minimizing the overall cost associated with the implementation and maintenance of these policies, ensuring a cost-effective approach to disease management. Furthermore, the numerical simulations that were conducted rigorously confirmed the beneficial and positive results stemming from the proposed control strategies, thereby validating their efficacy in curbing the spread of the coronavirus and managing its impact.

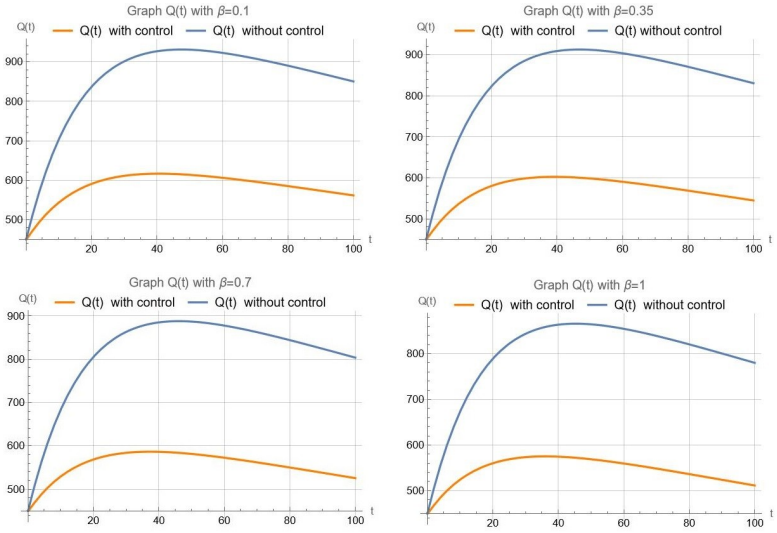

FIGURE 5. Comparison chart of $Q(t)$ in terms of parameter β with different values in uncontrolled and controlled systems.

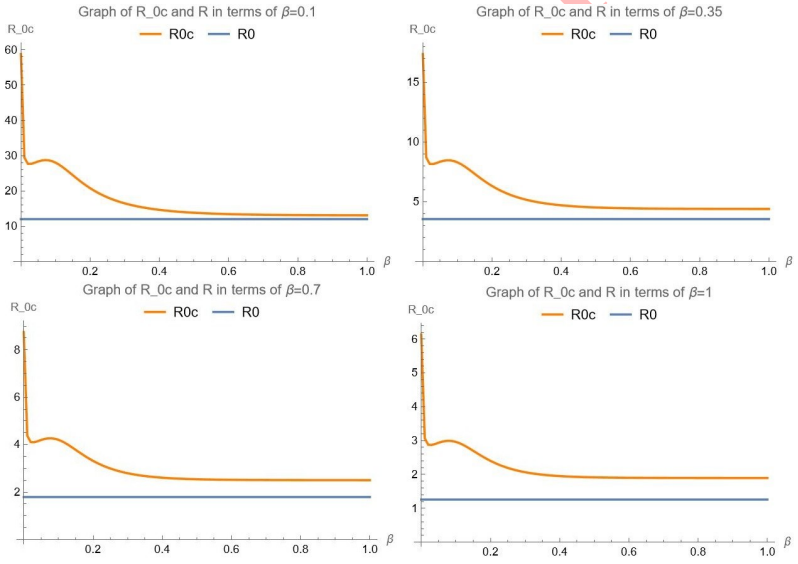

FIGURE 6. Comparison chart of the R_0 and R_0c in terms of parameter β with different values.

REFERENCES

[1] A. Abdullah, S. Ahmad, S. Owyed, A. H. AbdelAty, E. E. Mahmoud, K. Shah, and H. Alrabaiah, *Mathematical analysis of COVID-19 via new mathematical model*, Chaos, Solitons and Fractals, *143*(110585) (2021).

[2] W. E. Boyce and R. C. DiPrima, *Elementary Differential Equations and Boundary Value Problems*, John Wiley & Sons Canada Ltd., 2000.

[3] F. Bozkurt, A. Yousef, D. Baleanu, and J. Alzabut, *A mathematical model of the evolution and spread of pathogenic coronaviruses from natural host to human host*, Chaos Solitons Fractals, *138*(109931) (2020).

[4] K. Eikenberry, Y. Kuang, E. Kostelich, and A. B. Gumel, *To mask or not to mask: Modeling the potential for face mask use by the general public to curtail the COVID-19 pandemic*, Infectious Disease Modelling, *5* (2020), 293-308.
[5] P. D. En Ko, *On the course of epidemics of some infectious diseases*, Int J Epidemiol, *18*(4) (1989), 749-55.
[6] W. H. Fleming and R. W. Rishel, *Deterministic and Stochastic Optimal Control*, Springer, 1975.
[7] B. Isa Abdullahi, Y. Abdullahi, S. N. Kottakkaran, A. A. Abdel-Haleem, and A. T. Nofal, *Mathematical model to assess the imposition of lockdown during COVID-19 pandemic*, Results in Physics, *20*(103716) (2021).
[8] A. Kouidere, O. Balatif, H. Ferjouchia, A. Boutayeb, and M. Rachik, *Optimal Control Strategy for a Discrete Time to the Dynamics of a Population of Diabetics with Highlighting the Impact of Living Environment*, Discrete Dynamics in Nature and Society, *1*(6342169) (2019).
[9] S. S. Musa, S. Qureshi, S. Zhao, A. Yusuf, U. T. Mustapha, and D. He, *Mathematical modeling of COVID-19 Epidemic with effect of awareness programs*, Infectious disease modelling, *6* (2021), 448-460.
[10] L. S. Pontryagin, V. G. Boltyanskii, R. V. Gamkrelidze, and E. F. Mishchenko, *The Mathematical Theory of Optimal Processes*, Wiley, 1962.
[11] P. Van Den Driessche and J. Watmough, *Reproduction numbers and sub-threshold endemic equilibria for compartmental models of disease transmission*, Mathematical biosciences, *180*(1-2) (2002), 29-48.
[12] World Health Organization: (2019). www.who.int/emergencies/diseases/novel coronavirus.